International Journal of Nanomedicine

Dovepress
open access to scientific and medical research

Open Access Full Text Article

ORIGINAL RESEARCH

Amelioration effects of nanoencapsulated triterpenoids from petri dish-cultured *Antrodia cinnamomea* on reproductive function of diabetic male rats

This article was published in the following Dove Press journal:
International Journal of Nanomedicine

Sabri Sudirman
Yuan-Hua Hsu
Athira Johnson
David Tsou
Zwe-Ling Kong

Department of Food Science, National Taiwan Ocean University, Keelung City, Taiwan, Republic of China

Purpose: Nanoencapsulated triterpenoids from petri dish-cultured *Antrodia cinnamomea* (PAC) and its amelioration effects on reproductive function in diabetic rats were investigated.

Materials and methods: PAC encapsulated in silica–chitosan nanoparticles (Nano-PAC) was prepared by the biosilicification method. The diabetic condition in male Sprague Dawley rats was induced by high-fat diet and streptozotocin (STZ). Three different doses of Nano-PAC (4, 8, and 20 mg/kg) were administered for 6 weeks. Metformin and control of nanoparticles (Nano-con) were taken as positive and negative controls, respectively.

Results: The average particle size was ~79.46±1.63 nm, and encapsulation efficiency was ~73.35%±0.09%. Nano-PAC administration improved hyperglycemia and insulin resistance. In addition, Nano-PAC ameliorated the morphology of testicular seminiferous tubules, sperm morphology, motility, ROS production, and mitochondrial membrane potential. Superoxide dismutase (SOD), glutathione peroxidase (GPx), and catalase (CAT) antioxidant, as well as testosterone, luteinizing hormone (LH), and follicle stimulating hormone (FSH) were increased, whereas proinflammatory cytokines TNF-α, IL-6, and IFN-γ were decreased.

Conclusion: In the present study, we successfully nanoencapsulated PAC and found that a very low dosage of Nano-PAC exhibited amelioration effects on the reproductive function of diabetic rats.

Keywords: *Antrodia cinnamomea*, diabetes mellitus, insulin resistance, male reproduction, nanoparticles

Introduction

Diabetes mellitus (DM) is a metabolic disorder characterized by an increase in blood glucose (hyperglycemia) due to inadequate insulin production.[1] Oxidative stress and changes in antioxidant capacity are the major pathophysiological conditions that contribute to diabetes.[2,3] ROS is an oxygen-free radical and has a positive correlation with insulin resistance (IR) and cell dysfunction.[4] Several studies reported that hyperglycemia elevates the level of proinflammatory cytokines in the serum of the DM patient.[5,6] DM condition leads to the dysfunction of several organs such as testis, pancreas, and brain.[7,8] This disease has adverse effects on the reproductive function of diabetic human and experimental animal. For instance, DM causes adverse effects testosterone production,[9] impairs sperm motility, seminal fluid volume, and spermatogenesis with sperm deformities.[10] In DM patients, disorders in the endocrine control of spermatogenesis have also been observed with reduced levels of essential hormones, such as testosterone, luteinizing hormone (LH), and follicle stimulating

Correspondence: Zwe-Ling Kong
Department of Food Science, National Taiwan Ocean University, No. 2, Beining Road, Zhongzheng District, Keelung City 20224, Taiwan, Republic of China
Tel/fax +886 2462 2192 5130
Email kongzl@mail.ntou.edu.tw

submit your manuscript | www.dovepress.com
Dovepress
http://dx.doi.org/10.2147/IJN.S172906

hormone (FSH).[11,12] Diabetes mellitus was induced in an experimental animal by administration of streptozotocin (STZ), and it caused testicular degeneration and dysfunction.[13]

Modulation of hyperglycemia-induced oxidative stress represents an important strategy for the treatment of diabetes and its associated testicular dysfunction.[7] The initial recommendation for DM (especially type 2 diabetes mellitus [T2DM]) management approach includes lifestyle changes and monotherapy (usually with metformin [Met]).[14,15] Several oral agents have been used for DM treatment such as thiazolidinedione, insulin secretagogues (sulfonylureas and meglitinides), dipeptidyl peptidase-4 inhibitors, and alpha-glucosidase inhibitors (acarbose, miglitol, and voglibose).[16] Unfortunately, all antidiabetic agents have adverse effects. While considering Met, gastrointestinal-based side effects such as anorexia, nausea, abdominal discomfort, and diarrhea most frequently occur. Loss of efficacy and weight gain represent the main problems related to the use of sulfonylureas and meglitinides.[17] The other side effects of all sulfonylureas are headache, dizziness, nausea, hypersensitivity reactions, and weight gain.[18] Therefore, the investigation of novel antidiabetic agents, with less adverse effects and less cost, is a major challenge in the future research.

Antrodia cinnamomea (also called *Antrodia camphorata* or *Taiwanofungus camphoratus*) is a rare and unique fungus that is found in Taiwan.[19] *A. cinnamomea* is a medicinal mushroom widely applied in immune modulation, cancer prevention, and hepatoprotection in Asia and European over centuries.[20] Previous studies have shown that *A. cinnamomea* possesses immunomodulatory, anticancer,[21] and anti-obesity effects[22] and suppresses secretion of proinflammatory IL-1 and IL-18 as well as NLRP3 inflammasome activation in macrophages.[23] In addition, the triterpenoid compound eburicoic acid isolated from *A. cinnamomea* shows antidiabetic and antihyperlipidemia activities in palmitate-treated C2C12 myotubes and high-fat diet mice.[24] Triterpenoids are an important class of bioactive phytochemicals, the families of which are classified by differing quantities of structural isoprene units.[25] Despite the potential benefits, a primary limitation to the therapeutic use of phytochemicals including triterpenoids is low bioavailability through oral and systemic delivery.[26,27] Nanomaterials have recently been emerging as attractive pharmacological vehicles for drug delivery.[28] Nanocarriers with optimized physicochemical and biological properties are taken up by cells more easily than larger molecules, so they can be successfully used as delivery tools for currently available bioactive compounds.[29,30] In a nanoparticle (NP) form (encapsulated by chitosan/silica), the polysaccharides extracted from *A. cinnamomea* have been studied and had strong antioxidative activity as well as a potential role in cancer chemoprevention with antiproliferative effects in the cancer cell.[31] However, the effects of nanoencapsulated triterpenoids extracted from *A. cinnamomea* with silica–chitosan NPs on reproductive function in STZ-induced diabetic male rats have not been reported.

Therefore, the objective of this study was to characterize the properties of nanoencapsulated triterpenoids from petri dish-cultured *A. cinnamomea* (PAC) and to determine their amelioration effects on reproductive function in diabetic male rats.

Materials and methods

Materials

Chitosan was purchased from a commercial supplier (degree of deacetylation [DD]=81%, molecular weight [MW]=200 kDa). PAC ethanol extract was purchased from Kangli Company (Kaohsiung, Taiwan). Potassium dihydrogen phosphate was purchased from EMD Millipore (Billerica, MA, USA). Sodium silicate solution (Si=52%–57%) was purchased from Meru Chemical (Taipei, Taiwan). Acetic acid was purchased from Zhenyuan Chemical (Taipei, Taiwan). FBS and Roswell Park Memorial Institute (RPMI) 1640 were purchased from Thermo Fisher Scientific (Waltham, MA, USA). Met 500 mg was purchased from TCM Biotech International Corp. (Taipei, Taiwan). Formalin was purchased from Macron Fine Chemicals (Center Valley, PA, USA). The FSH ELISA kits, LH ELISA kits, and testosterone ELISA kits were purchased from MyBioSource (San Diego, CA, USA). The IFN-γ ELISA and IL-6 ELISA kits were purchased from Koma Biotech (Seoul, Korea). The TNF-α ELISA kits were purchased from Abcam (Cambridge, UK). Insulin ELISA kit was purchased from Mercodia AB (Uppsala, Sweden).

Preparation of triterpenoids from PAC encapsulated in silica–chitosan nanoparticles (Nano-PAC)

Nano-PAC triterpenoids were prepared by using sodium silicate and chitosan solution.[31] Sodium silicate was dissolved in 0.05 M sodium acetate to prepare 0.7% (w/w) solution (pH=5.6). Chitosan was dissolved in 0.1 M acetic acid to prepare 0.7% (w/w) solution (pH=5.6). Then, 10 mL of sodium silicate (0.7% w/w), 1 mL of PAC in 95% alcohol solution (0.2% w/v), and 1 mL of chitosan solution (0.7% w/w) were added together and mixed completely. Afterward, the

suspensions were centrifuged at 20,000 × *g* for 30 minutes. Finally, NPs were freeze-dried into powder (Nano-PAC).

Particle size, size distribution, and surface charge of Nano-PAC measurement

Nano-PAC was diluted 1,000 times in deionized water and further filtered with 0.22 μm membranes. Each 700 μL of sample was placed in a quartz tube and measured for the averaged particle diameter and zeta potential by Zetasizer nano range (Malvern Instruments, Malvern, UK). Hitachi S-4800 scanning electron microscope (SEM; Hitachi Ltd., Tokyo, Japan) was used to observe the particle size and morphology of NPs, and the micrographs were taken at 15 kV.[31]

Encapsulation efficiency (EE) and loading capacity

The EE of NPs was measured by HPLC.[32] A C18 reversed-phase column was used, and the column effluent was detected at 280 nm with a UV/Vis detector. The sample was dissolved in ethanol and then extracted by mobile phase. The standard curve was drawn manually. The concentration value of PAC was taken as abscissa and the integration area as the vertical coordinate. The calculation equation is as follows:

$$\text{EE}\ (\%) = \frac{\text{Total amount of PAC} - \text{Free PAC in the supernatant}}{\text{Total amount of PAC}} \times 100\%$$

$$\text{Loading capacity}\ (\%) = \frac{\text{Total amount of PAC} - \text{Free PAC in the supernatant}}{\text{Weight of the NPs}} \times 100\%$$

In vitro drug release

The nanoencapsulated particles were exposed to simulated gastric fluid (SGF) and simulated intestinal fluid (SIF) according to the procedure described by Maiti et al.[33] SGF was prepared as described in the United States Pharmacopeia and consists of 3.2 mg/mL of pepsin in 0.03 M NaCl at pH 1.2. SIF was prepared as described in the United States Pharmacopeia and consisted of 10 mg/mL of pancreatin in 0.05 M KH_2PO_4, pH 6.8. Freeze-dried drug-loaded NPs (2%) were put into 100 mL of SGF at 37°C with stirring. During the test, aliquots of digest were withdrawn at specific time intervals (0, 5, 10, 15, 20, 30, 45, 60, 90, and 120 minutes), and the reaction was stopped by cooling in ice. After the gastric test, the system was centrifuged at 20,000 × *g* for 30 minutes. The pellets were collected into SIF at 37°C with stirring. Aliquots of digest were withdrawn at specific time intervals (0, 5, 15, 30, 45, 60, 90, 120, 180, and 240 minutes). At different time intervals, the drug release in the fluid was determined by HPLC at 280 nm. The release profiles were fitted as follows:

$$\text{Release}\ (\%) = \frac{A_S}{A_T} \times 100\%$$

Here, A_T is the absolute amount of PAC at infinite time and A_S is the release amount of PAC at specific time intervals.

Cell viability and anti-inflammation assay on LC540 cell line

Cell culture

Rat testis Leydig tumor cell line (LC540) was purchased from Food Industry Research and Development Institute (FIRDI) (Hsinchu, Taiwan) and cultured in DMEM/F12, containing 2 mM of L-glutamine, 0.1 mM of nonessential amino acids (NEAA), 1.5 g/L of sodium pyruvate, 100 U/mL of penicillin, and 10% of FBS. The cells were maintained at 37°C in a humidified atmosphere (5% CO_2).

Cell viability

Cell viability was performed by using an MTT-based colorimetric assay as described in the previous method.[34] Briefly, LC540 cells were cultured with Nano-PAC or without Nano-PAC (control) for 24 hours, and then the cell culture supernatant was removed and washed with PBS. Then, MTT solution (1 mg/mL) was added and incubated for 4 hours. After incubation, the cells were dissolved in dimethyl sulfoxide (DMSO), and the absorbance was measured using an ELISA reader at 570 nm. The cell viability was expressed as percentage of control.

Nitric oxide (NO) production and anti-inflammation assay

The scavenging potential for superoxide radicals was determined via nitro blue tetrazolium (NBT) reduction, which measured the NO on the cell supernatant.[35] The LC540 cells were cultured with or without Nano-PAC and lipopolysaccharides (LPS; 10 μg/mL) for 24 hours, and the cell supernatant was transferred into the new well for NO analysis. Then, NBT solution was added (1 mg/mL of NBT, 5% of FBS, 3% of DMSO in 10 mL of DMEM/F12) and incubated for 1 hour and centrifuged to remove the supernatant. Afterward, it was dissolved in DMSO, and the absorbance was measured by using the ELISA reader at 570 nm. For NO analysis, the cell culture supernatants were mixed with NO

solution (sulfanilamide and *N*-(1-naphthyl)ethylenediamine dissolved in 5% H_3PO_4 and H_2O, respectively, and mixed in the volume ratio 1:1 immediately before use) for 10 minutes. Afterward, the absorbance was measured by using the ELISA reader at 540 nm.

STZ-induced diabetic male rats

All the procedures were carried out according to the Animal Protection Act (Act/APC) and the Experimental Animal Ethics Committee of the Council of Agriculture (CoA) of the Executive Yuan, Taiwan. The Institutional Animal Care and Use Committee (IACUC; Approval No 106016) of the National Taiwan Ocean University reviewed and approved all protocols. Male Sprague Dawley rats (5-week-old) were purchased from the BioLASCO Taiwan Co., Ltd. (Yilan, Taiwan). The animals were housed under standard laboratory conditions (temperature, 23°C±1°C), 40%–60% humidity; 12:12 light:dark cycle) in cages.

First, the rats were divided into control (Con) group (n=9) and diabetic group (n=54); the Con group was fed with the standard rodent chow, and the diabetic group was fed with the high-fat diet (40% calories made by lard) for 3 weeks. A single subcutaneous injection of STZ (35 mg/kg in 0.1 M citrate buffer, pH=4.5) was made to induce diabetes in rats. After 1 week, oral glucose tolerance test (OGTT) was carried out by orally administering glucose (2 g/kg) after 12 hours of fasting and blood was drawn to measure glucose levels at 0, 30, 60 and 120 minutes after glucose injection.

Then, the rats were divided into seven groups (n=8) as follows: Group 1, control rats; Group 2, diabetic rats; Group 3, Nano-PAC1-treated diabetic rats (4 mg/kg/day); Group 4, Nano-PAC2-treated diabetic rats (8 mg/kg/day); Group 5, Nano-PAC5-treated diabetic rats (20 mg/kg/day); Group 6, Met-treated diabetic rats (300 mg/kg/day); and Group 7, Nano-control-treated diabetic rats (20 mg/kg/day). Rats were intragastric administered for 6 weeks, and then OGTT was conducted before sacrificed.

Glucose and insulin assay

The plasma glucose concentration was tested by glucose enzymatic kits (Randox, Crumlin, UK). Plasma insulin concentration was tested by insulin ELISA kits.

Testis tissue collection and homogenization

From each animal, one testis was stored at −80°C and the other one was soaked in formalin. Five-micrometer-thick paraffin sections were cut and send to Rapid Science Co., Ltd., for H&E staining. In addition, tissue slices were taken and washed in PBS and homogenized in PBS. Then, they were freezed and thawed twice. After the blending process, they were centrifuged at 5,000 rpm. The supernatant was collected and stored at −80°C.[36]

Sperm parameters

The swim-up method was used to collect sperm from epididymides.[37] The epididymides were cut in the RPMI medium and shaked for 100 rpm. After that, they were centrifuged at 100 × *g* and incubated at 37°C in 5% CO_2 incubator. Finally, the sperm was collected from the supernatant and observed under a microscope to observe sperm count, motility, and abnormality.

Oxidative stress assay

The superoxide dismutase (SOD), glutathione peroxidase (GPx), and catalase (CAT) activities were used to evaluate antioxidative activity in testis and were tested by using Randox kit. Malondialdehyde (MDA) levels were used to evaluate lipid peroxidation. Testis homogenate and plasma were mixed with the reactive solution (15% [w/v] trichloroacetic acid in 0.25 *n*-HCl and 0.375% (w/v) thiobarbituric acid in 0.25 *n*-HCl) and placed in 100°C water bath for 15 minutes. After cooling, the mixture was added to 300 µL *n*-butanol and was centrifuged at 1,500 × *g* for 10 minutes. The clear supernatant was measured at the 532 nm absorbance.

Anti-inflammation and endocrine system analysis

TNF-α, IFN-γ, and IL-6 in plasma and testis were detected by enzyme-linked immunosorbent assay. LH, FSH, and testosterone regulated the reproductive endocrine system, and all of them were detected by ELISA in plasma and testis.

JNK-signaling-related protein

The protein expressions of JNK signaling pathway such as ASK1, c-Jun, and ATF2 were determined by ELISA, and the assays were performed according to the manufacturer's protocols.

Sperm ROS production and mitochondrial membrane potential (MMP) level

The level of ROS of the sperm was determined by probe 2′,7′-dichlorofluorescein-diacetate (DCFH-DA) staining method as described by previous methods.[38] The DCFH-DA

method is commonly used as a probe to detect the formation of ROS. Flow cytometry (BD FACSAria; BD Biosciences, San Jose, CA, USA) was used to quantify the fluorescence at the single-cell level. A minimum of 10^6 sperms/mL were examined for each assay. One milliliter of the sperm fraction was loaded with the stain DCFH-DA and incubated for 30 minutes at 37°C and then centrifuged at 800 × *g* for 3 minutes in the dark. After washing the cells twice with PBS (5 minutes), the conversion of DCFH to dichlorofluorescein (DCF) was observed, which had a green fluorescent (DCF-DA) color that was detected and evaluated between 500 and 530 nm by flow cytometry.

The changes in MMP were estimated by using the fluorescent cationic dye rhodamine 123 (Rh 123), which accumulates electrophoretically in mitochondria as a direct function of the membrane potential and is released upon membrane depolarization as described by the previous method.[39] The sperms (10^6 cells/mL) were preincubated with Rh 123 for 30 minutes at 37°C. A sample of the cell suspension (1 mL) was transferred to a fluorometer cuvette, and the change in fluorescence at excitation and emission wavelengths of 505 and 525 nm, respectively, at 30°C was recorded continuously using a flow cytometry (BD FACSAria) with thermostatically controlled cuvette with magnetic stirring.

Statistical analyses

Data are reported as mean value of at least three replicates. Statistical analyses by Duncan's multiple range tests ($P<0.05$) were conducted using SPSS 22.0 (IBM Corporation, Armonk, NY, USA) software to analyze the experimental data. All data were expressed as mean±SD.

Results and discussion

Characteristics of Nano-PAC

The effect of concentration of chitosan and silica solution on preparation of Nano-PAC was evaluated by measuring the diameter, zeta potential, EE, and loading capacity of NPs (Table 1). The controlled release and morphology of Nano-PAC are shown in Figure 1. The morphology of Nano-PAC was spherical in shape. As a comparison, the previous study reported that the particle size and EE on *A. camphorata* extract (ACE) polysaccharides encapsulated in silica–chitosan were 294±26 nm and 63.5%, respectively.[31] The results confirm the smaller size and high EE of triterpenoids in chitosan–silica NPs. Both synthesis process and environmental parameters such as conductivity, polymer MW, surface tension, polymer concentration, and acid concentration were affected by the size of NPs.[40] We hypothesized that the small size of the Nano-PAC was due to the fabrication process and the electrostatic interaction between the silica, chitosan, and PAC.

Table 1 The characteristic of Nano-PAC

Parameter	Particle size (nm)	Zeta potential (mV)	EE (%)	Loading capacity (%)
Nano-PAC	79.46±1.63	−11.4±1.45	73.35±0.09	50.66±0.32

Note: Data are shown as mean±SD (n=3).
Abbreviations: Nano-PAC, PAC encapsulated in silica–chitosan nanoparticles; EE, encapsulation efficiency; PAC, petri dish-cultured *Antrodia cinnamomea*.

Cellular uptake of NPs is affected by the NP size, surface charge, shape, and surface coating of NPs.[41–43] Smaller particles have a higher surface area-to-volume ratio, which makes it easier for the encapsulated drug to release from the NPs via diffusion, and surface erosion added advantage to permeate through the physiological drug barriers.[32] The distinct feature of NPs is their unique size, which allows them to enter the cells and can reach to the genetic material by crossing the nuclear membrane because of the smaller size, allowing them more contact with the biological membranes.[44,45] In addition, smaller NPs will have greater ease of entry and durability in the tumors.[46] The NPs can be entered into the cells by the mechanism called endocytosis. The process of endocytosis is divided into three types called phagocytosis (cellular eating), pinocytosis (cellular drinking), and receptor-mediated endocytosis.[45,47] Because of the small size, the Nano-PAC can enter the cells via the abovementioned three processes.

Surface charge can also influence the cellular uptake process. Surface charge property of an object in contact with an aqueous solution plays a very important role in the applications of surface science, colloidal science, and electrokinetic transport.[41] SiO^- ion dissociated from the functional group SiOH[41,48] and negative charge from triterpenoids interact with positive charge from chitosan (NH_3^+), yielding lower negative surface charge density in the interaction region. Nano-PAC with negative surface charge can interact with the positive charge of the substrate.

NPs have been demonstrated to possess great potential for enhancing drug delivery.[49] EE is an important index for active ingredient or drug delivery systems, especially true for expensive drugs.[32] Silica–chitosan NPs have high efficiency to encapsulate triterpenoids from *A. cinnamomea* (73.35%). A previous study showed the EE of ACE polysaccharides in silica–chitosan was 63.5%.[31] The EE of triterpenoids by silica–chitosan NPs is probably due to electrostatic

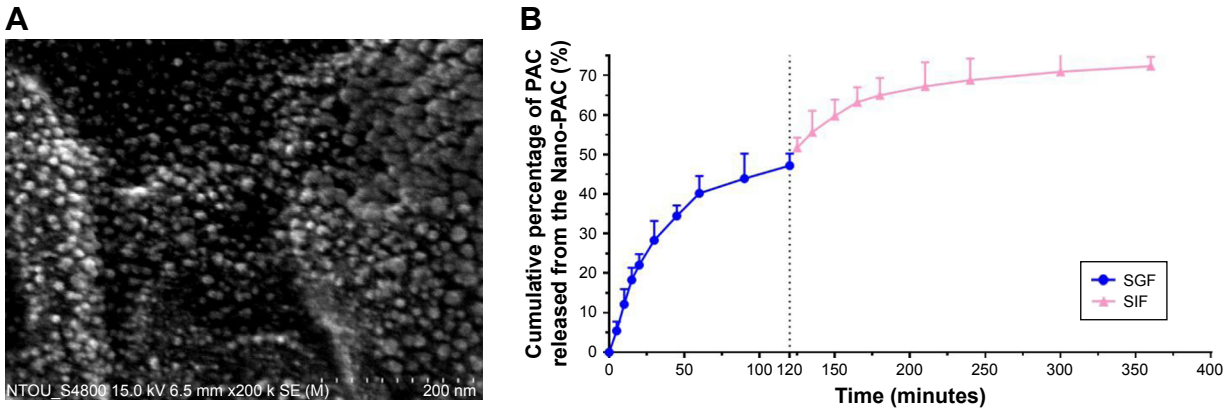

Figure 1 The characteristic of Nano-PAC: (**A**) spherical shapes showed by scanning electron microscopy and (**B**) control release.
Abbreviations: Nano-PAC, PAC encapsulated in silica–chitosan nanoparticles; PAC, petri dish-cultured *Antrodia cinnamomea*; SGF, simulated gastric fluid; SIF, simulated intestinal fluid.

interaction mechanism between triterpenoids and the NPs: the electrostatic interaction with chitosan.

The shape of the nanocarriers has been identified as one of the key factors that influences crucial physiological processes, including cellular uptake and specific cellular targeting.[50,51] In this study, the Nano-PAC shows the spherical shape. Spherical NPs have been widely used as vehicles for drug delivery.[52] In addition, rod-shaped capsules were taken up by HeLa cells to a lower extent compared with spherical capsules.[53]

Cell viability of LC540 cell

The cell viability of rat testis Leydig tumor cell (LC540) after treating by different concentrations of Nano-PAC was measured by MTT assay. Figure 2 shows that the cell viability of 19.53–312.50 μg/mL of Nano-PAC was ≥90%, and the cell viability was decreased with an increase in concentration. A previous study reported that ACE polysaccharides encapsulated in silica and silica–chitosan NPs decreased the viability of human cancer cell line but not of the normal cell line.[31]

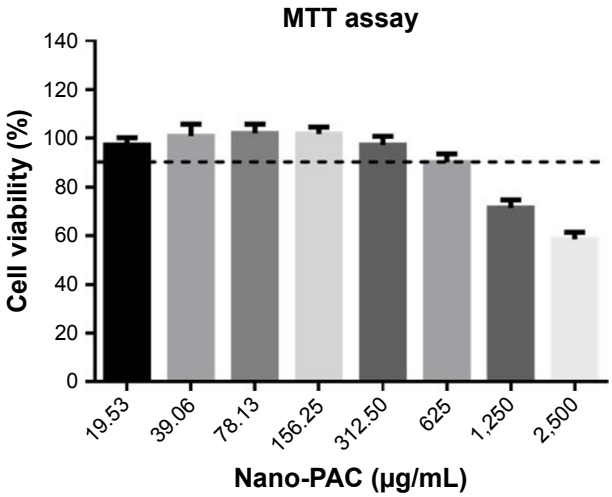

Figure 2 Cell viability of LC540 cell after treating with Nano-PAC for 24 hours.
Note: Data are shown as mean±SD (n=3).
Abbreviations: Nano-PAC, PAC encapsulated in silica–chitosan nanoparticles; PAC, petri dish-cultured *Antrodia cinnamomea*.

NO and superoxide production

Treatment with Nano-PAC for 24 hours on LC540 cell significantly ($P<0.05$) decreased the NO and superoxide anion (O_2^-) production induced by LPS (Figure 3). Production of ROS is central to the progression of many inflammatory diseases. NO is considered as a proinflammatory mediator that induces inflammation due to over production in abnormal situations.[54,55] A previous study reported that *A. cinnamomea* ethanol extract suppressed the ROS or superoxide production in human acute monocytic leukemia THP-1 cell induced by LPS and extracellular adenosine 5′-triphosphate (ATP).[23]

Fasting blood glucose level, insulin level, and homeostasis model assessment-estimated insulin resistance (HOMA-IR) in rat plasma

Oral supplementation of Nano-PAC into STZ-induced diabetic rats ameliorated the higher fasting blood glucose as stated for the diabetic group. The diabetic group showed a significant ($P<0.05$) increased plasma insulin and HOMA-IR in comparison with Con and Nano-PAC groups as well as the Met group (Table 2). The increased insulin levels in the current study were in agreement with the findings by Chang and Kwon[56] and Pandya et al[57] who reported the same in STZ-induced diabetic rats.

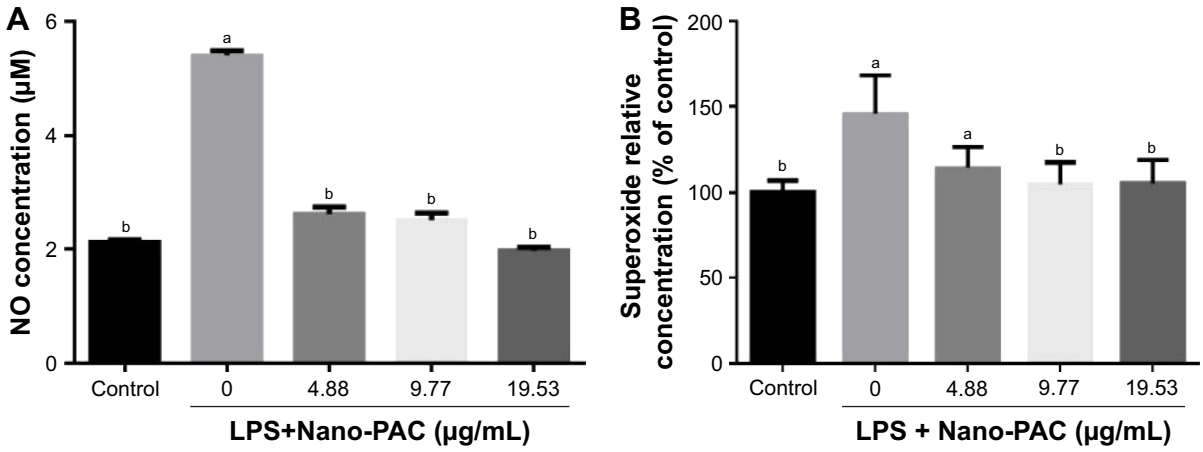

Figure 3 Effect of Nano-PAC on (**A**) NO and (**B**) superoxide production of LC540 cell after treating for 24 hours, induced by LPS (10 μg/mL).
Notes: Data are shown as mean±SD (n=3). The values with different letters (a and b) represent significant ($P<0.05$) difference as analyzed by the Duncan's multiple range test.
Abbreviations: Nano-PAC, PAC encapsulated in silica–chitosan nanoparticles; NO, nitric oxide; LPS, lipopolysaccharides; PAC, petri dish-cultured *Antrodia cinnamomea*.

Determination of fasting glucose (fasting plasma blood glucose) level is a biomarker for diagnosis of diabetes. The current study showed that diabetic rats had a significant increase in fasting glucose and increase in the insulin level when matched with Con and Nano-PAC5-treated groups and had similarity with previous a report stating that Antcin K (a triterpenoid compound from *A. camphorata*) reduced the blood glucose and insulin level.[58] In addition, dehydroeburicoic acid[59] and eburicoic acid[24] (triterpenoid compound from *A. camphorata*) prevented diabetes by the regulation of GLUT4 and AMP-activated protein kinase phosphorylation in STZ-induced diabetic mice.

The HOMA-IR has been widely used for the estimation of IR.[60] IR is a feature of disorders such as T2DM and is characterized by increasing the concentration of insulin.[61,62] HOMA-IR was calculated by multiplying fasting plasma glucose by fasting plasma insulin and dividing by 22.5.[63] The levels of circulating insulin and plasma glucose were directly proportional to the HOMA-IR level and vice versa. In this study, the HOMA-IR level ameliorated by the administration of Nano-PACs from diabetic condition was the same as that of the Con group. Administrating by Nano-PACs showed that the HOMA-IR level was lower when compared with several cutoff levels for IR. Several studies showed that the cutoff level of HOMA-IR for identifying those with IR is 2.77 for Brazilians,[63] 2.22–3.16 for Indian Adolescents,[64] and 3.80 for American-Hispanic population.[60]

Testis, epididymis, and epididymal adipose weight

Oral administration of Nano-PAC5 significantly ($P<0.05$) improved the testis, epididymis, and epididymal adipose weights when compared with those of the diabetic (DM) group. Furthermore, there were no significant differences between Nano-PAC5-treated rats and the Con group (Table 3).

The weights of testis and epididymis were decreased in diabetic rats, and this may be attributed to the testicular deterioration and decline in the epididymis weight. In addition, the atrophic alterations in the epididymis are due to reduced tubular diameter, volume, and surface density in

Table 2 Plasma fasting blood glucose level, plasma insulin level, and HOMA-IR in STZ-induced diabetic rats fed different doses of Nano-PAC after 42 days

Parameters	Con	DM	Nano-PAC1	Nano-PAC2	Nano-PAC5	Met	Nano-con
Fasting glucose (mg/mL)	91.43±0.31^b	251.15±0.68^a	145.31±0.27^b	124.98±0.32^b	95.67±0.31^b	99.13±0.28^b	298.88±0.62^b
Insulin (μg/L)	0.31±0.01^b	0.68±0.18^a	0.27±0.01^b	0.32±0.02^b	0.31±0.02^b	0.28±0.01^b	0.62±0.02^b
HOMA-IR	2.02±0.19^b	12.88±3.88^a	2.79±0.40^b	2.86±0.49^b	2.14±0.13^b	1.96±0.20^b	13.29±1.35^b

Notes: Data are shown as mean±SD (n=6 rats/group). The values with different letters (a and b) represent significant ($P<0.05$) difference as analyzed by the Duncan's multiple range test. The HOMA-IR=fasting plasma glucose (mmol/L)×fasting plasma insulin (mU/L)/22.5.
Abbreviations: HOMA-IR, homeostasis model assessment-estimated insulin resistance; STZ, streptozotocin; Nano-PAC, PAC encapsulated in silica–chitosan nanoparticles; Con, control; DM, diabetes mellitus; Nano-PAC1, diabetes+4 mg/kg per day Nano-PAC; Nano-PAC2, diabetes+8 mg/kg per day Nano-PAC; Nano-PAC5, diabetes+20 mg/kg per day Nano-PAC; Met, diabetes+300 mg/kg per day metformin; Nano-con, diabetes+20 mg/kg per day silica–chitosan nanoparticles; PAC, petri dish-cultured *Antrodia cinnamomea*.

Table 3 The testis, epididymis, and epididymal adipose weight (% of body weight) in STZ-induced diabetic rats fed different doses of Nano-PAC after 42 days

Testis and adipose weight (% of body)	Con	DM	Nano-PAC1	Nano-PAC2	Nano-PAC5	Met	Nano-con
Testis	0.84±0.03[a]	0.74±0.03[b]	0.80±0.03[a,b]	0.81±0.03[a,b]	0.86±0.04[a]	0.89±0.03[a]	0.74±0.02[b]
Epididymis	0.30±0.01[a]	0.28±0.01[b]	0.30±0.01[a]	0.29±0.01[a,b]	0.31±0.01[a]	0.32±0.01[a]	0.27±0.01[b]
Epididymal adipose	1.22±0.05[a]	1.57±0.12[a]	1.22±0.10[b]	1.28±0.04[b]	1.27±0.04[b]	1.10±0.10[b]	1.57±0.10[a]

Notes: Data are shown as mean±SD (n=6 rats/group). The values with different letters (a and b) represent significant ($P<0.05$) difference as analyzed by the Duncan's multiple range test.

Abbreviations: STZ, streptozotocin; Nano-PAC, PAC encapsulated in silica–chitosan nanoparticles; Con, control; DM, diabetes mellitus; Nano-PAC1, diabetes+4 mg/kg per day Nano-PAC; Nano-PAC2, diabetes+8 mg/kg per day Nano-PAC; Nano-PAC5, diabetes+20 mg/kg per day Nano-PAC; Met, diabetes+300 mg/kg per day metformin; Nano-con, diabetes+20 mg/kg per day silica–chitosan nanoparticles; PAC, petri dish-cultured *Antrodia cinnamomea*.

diabetic rats.[65] Testicles and other reproductive tissues depend upon testosterone, which motivates growth and secretary action of the reproductive organs.[66] Oral treatment of Nano-PACs significantly decreased the epididymal adipose weight compared with that in the diabetic group. The adipose tissue is highly involved in the development of metabolic disorders such as cardiovascular disease (CVD) and T2DM.[67]

The seminiferous tubule structure in STZ-induced diabetic rats group appeared shrunken and separated from each other (Figure 4B) compared with other treatments (Figure 4A, C, and D). Histopathological observation showed that STZ caused obvious seminiferous tubule degeneration. Male fertility depends on the continual renewal of spermatogonia and their differentiation into spermatogenic cells.[68] In diabetic rats, seminiferous tubule diameter was found to be decreased; basement membrane was found to be thickened in seminiferous tubules, and the degenerated germ cell was also seen.[69] In addition, Orman et al[68] reported an

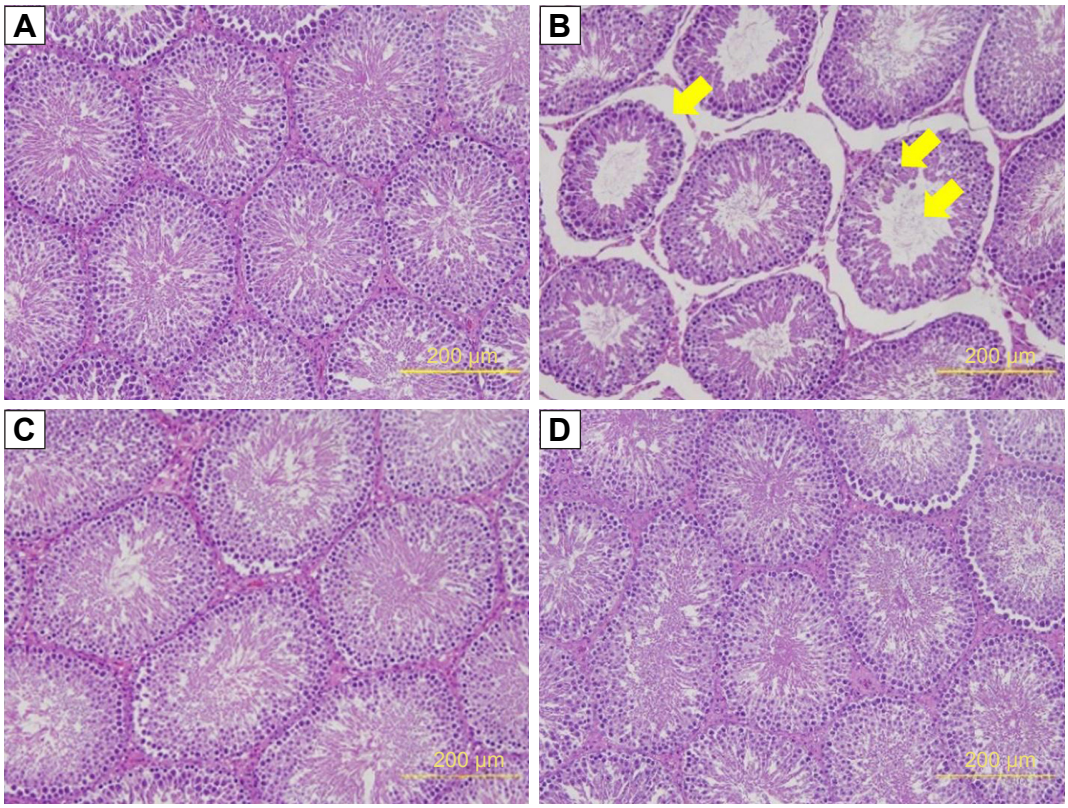

Figure 4 Thickness of seminiferous tubule in STZ-induced diabetic rats: (**A**) Con, (**B**) DM, (**C**) Nano-PAC5, and (**D**) Met.

Notes: The testis sections were stained with H&E. The yellow arrow indicates the changes in the seminiferous tubule.

Abbreviations: STZ, streptozotocin; Con, control; DM, diabetes mellitus; Nano-PAC5, diabetes+20 mg/kg per day Nano-PAC; Met, diabetes+300 mg/kg per day metformin; Nano-PAC, PAC encapsulated in silica–chitosan nanoparticles; PAC, petri dish-cultured *Antrodia cinnamomea*.

atrophy of the seminiferous tubules and a dissociation with tubular shedding of immature spermatogenic cells in the diabetic model. Oral supplementation of Nano-PAC5 had amelioration effects on tubular diameter by stimulating cell survival and spermatogenesis due to Nano-PAC5-mediated alleviation of oxidative stress.

SOD, GPx, and CAT antioxidant in testis

The results showed a significant decrease ($P<0.05$) in the level of SOD, GPx, and CAT antioxidants in the testis of the diabetic (DM) group when compared with Con and Nano-PAC5 groups (Figure 5). Nano-PAC-treatment had an ameliorated effect on primary antioxidant activity in STZ-induced diabetic rats.

In this study, diabetic rats showed a decrease in SOD, GPx, and CAT activities. Hyperglycemia is known to reduce the activity of SOD in the sciatic nerve of the animal,[5] increase glycolysis, activate the intracellular sorbitol (polyol) pathway, and increase free radical formation.[68] SOD protects biological tissues from highly reactive superoxide anions (O_2^-) by converting them to H_2O_2, whereas CAT plays a role in the catalytic decomposition of harmful H_2O_2 to O_2 and H_2O. In the absence of breakdown by CAT or GPx, Hydrogen peroxidase (H_2O_2) lead to the production of reactive hydroxyl radicals, reduce the cellular protection and make tissues easier to attack by free radicals. Several studies reported that SOD, GPx, and CAT were decreased in diabetic rat model.[5,68,70,71] In the present study, the Nano-PAC5-treated STZ-induced diabetic rats inhibited the oxidative stress by increasing the antioxidant activities of SOD, GPx, and CAT.

TNF-α, IL-6, and IFN-γ

The testicular IL-6 and TNF-α expression levels were significantly lower ($P<0.05$) in Con and Nano-PAC-treated groups (Figure 6). Nano-PAC5 group showed significantly decreased ($P<0.05$) plasma IFN-γ production, and it returned to the same level as the Con group.

The DM group was accompanied by the overexpression of IL-6, TNF-α, and IFN-γ. These are proinflammatory cytokines that mediated reproductive dysfunction by generating testicular injuries that lead to testicular atrophy and apoptosis.[1,72] Several authors reported the increase in the level of proinflammatory cytokines of diabetic rats such as TNF-α, IL-1β, IL-6, IFN-γ, and NF-κB.[5,7,72,73] These inflammatory cytokines are involved in systemic inflammation and stimulation of acute-phase reaction, and the elevated levels of these inflammatory mediators are found to be a consequence of hyperglycemia and IR in diabetes.[74,75] The levels of IL-6, TNF-α, and IFN-γ decreased by Nano-PAC treatment in the present study.

Expression of protein-related JNK signaling pathways

The protein expression levels of JNK pathways such as ASK1, c-Jun, and ATF2 were increased in the diabetic condition (Figure 7). A previous study reported that the overexpression of ASK1 was associated with IR,[76] and the LPS and ROS are the key cellular stressors that activate the ATF2.[77] Phosphorylation process is required for the activation of ATF2 and is mediated by some protein expression including JNK,[78] which is known as the most investigated signal transducer in obesity and IR.[79] Our results

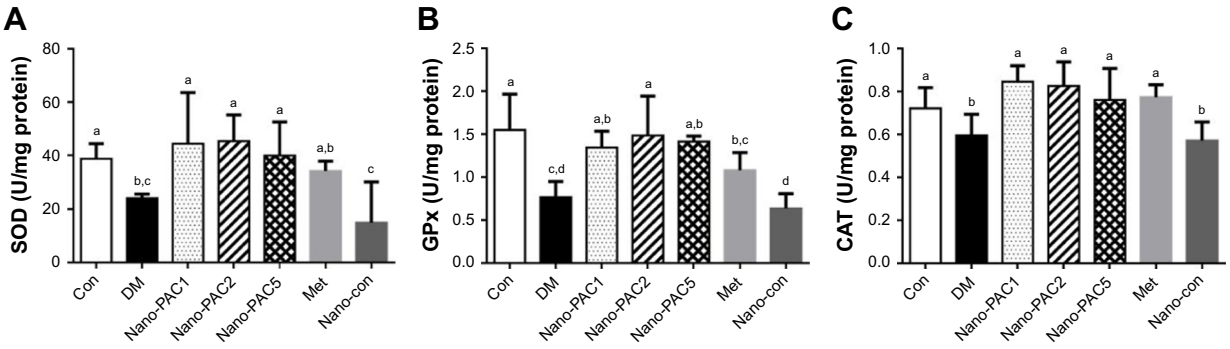

Figure 5 Activity of (**A**) SOD, (**B**) GPx, and (**C**) CAT in testis of STZ-induced diabetic rats fed different doses of Nano-PAC after 42 days.

Notes: Data are shown as mean±SD (n=6 rats/group). The bars with different letters (a–d) represent significant ($P<0.05$) difference as analyzed by the Duncan's multiple range test.

Abbreviations: SOD, superoxide dismutase; GPx, glutathione peroxidase; CAT, catalase; STZ, streptozotocin; Nano-PAC, PAC encapsulated in silica–chitosan nanoparticles; Con, control; DM, diabetes mellitus; Nano-PAC1, diabetes+4 mg/kg per day Nano-PAC; Nano-PAC2, diabetes+8 mg/kg per day Nano-PAC; Nano-PAC5, diabetes+20 mg/kg per day Nano-PAC; Met, diabetes+300 mg/kg per day metformin; Nano-con, diabetes+20 mg/kg per day silica–chitosan nanoparticles; PAC, petri dish-cultured *Antrodia cinnamomea*.

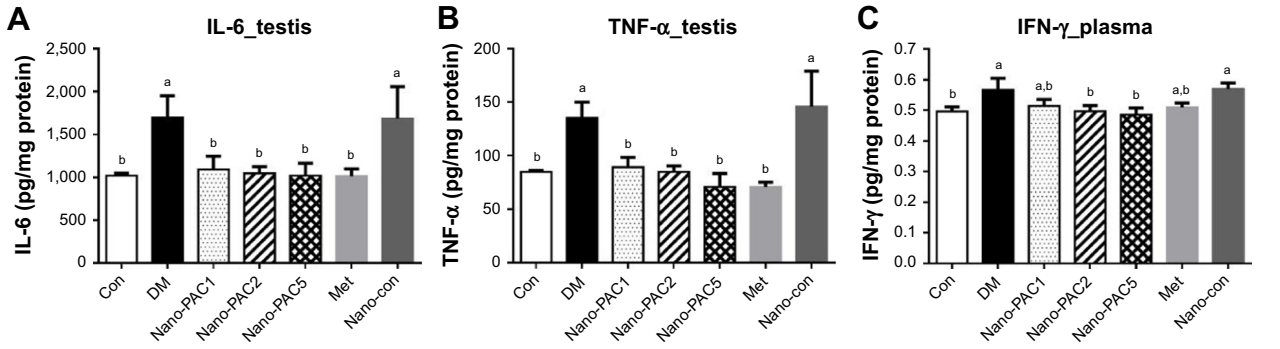

Figure 6 Testis (**A**) IL-6 and (**B**) TNF-α and (**C**) plasma IFN-γ production in STZ-induced diabetic rats fed different doses of Nano-PAC after 42 days.
Notes: Data are shown as mean±SD (n=6 rats/group). The bars with different letters (a and b) represent significant ($P<0.05$) difference as analyzed by the Duncan's multiple range test.
Abbreviations: STZ, streptozotocin; Nano-PAC, PAC encapsulated in silica–chitosan nanoparticles; Con, control; DM, diabetes mellitus; Nano-PAC1, diabetes+4 mg/kg per day Nano-PAC; Nano-PAC2, diabetes+8 mg/kg per day Nano-PAC; Nano-PAC5, diabetes+20 mg/kg per day Nano-PAC; Met, diabetes+300 mg/kg per day metformin; Nano-con, diabetes+20 mg/kg per day silica–chitosan nanoparticles; PAC, petri dish-cultured *Antrodia cinnamomea*.

show that the treatment with Nano-PAC has downregulated the expression of these proteins and thereby increased the insulin sensitivity.

Sperm parameters

Figure 8 shows that the amelioration effects of Nano-PAC treatment on STZ-induced diabetic rats. Nano-PAC5 treatment had significantly increased and decreased ($P<0.05$) the sperm mobility and abnormality, respectively. The sperm morphology using light microscopy is shown in Figure 9. The diabetic (DM) group showed more abnormal sperm (Figure 9B) than other treatment groups.

The decrease in sperm mobility may be due to structural and functional changes during sperm tail morphogenesis as diabetes is known to induce sperm abnormalities.[80] The recovery of sperm counts and motility, as well as reduction in abnormality of Nano-PAC-treated diabetic rats, can be attributed to antioxidant properties of triterpenoids in Nano-PACs. Triterpenoids have shown protective effects against free radicals because of their antioxidant properties.[81,82]

Sperm ROS production and MMP level

Control and Nano-PAC5 treatment in STZ-induced diabetic rats exhibited lower ROS production and higher MMP in sperm compared with the diabetic (DM) group (Figure 10). The lower level of sperm ROS in Nano-PAC treatment in STZ-induced diabetic rats showed that Nano-PAC has potent ameliorative properties against ROS development and acts as a free radical scavenger. The reduction in oxidative stress biomarkers may be also due to the inhibition of hyperglycemia as it has been recognized to trigger oxidative stress and to be involved in the pathogenesis of DM.[5] Triterpenoid from the *A. cinnamomea* extract showed to possess antioxidant properties against free radicals.[82] In addition, ACE polysaccharide-encapsulated silica–chitosan NP has a high scavenging activity.[31] On the other hand, the MMP level

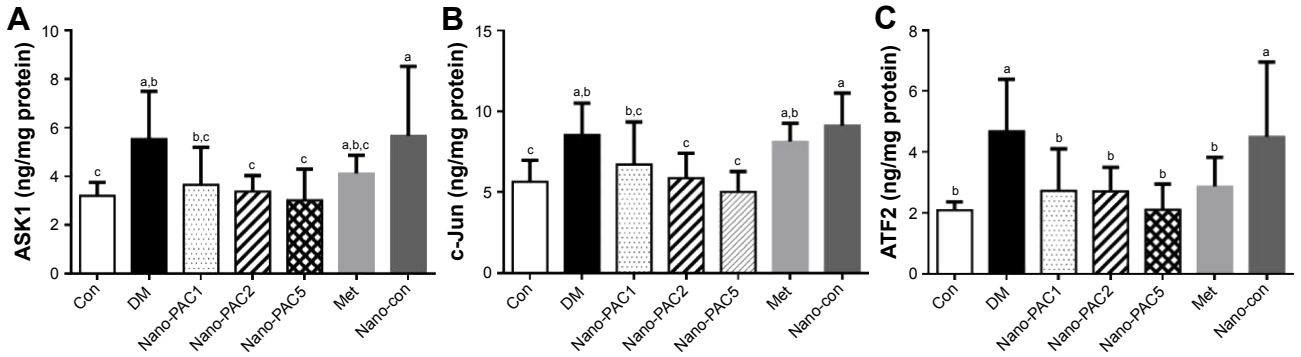

Figure 7 Protein expression of (**A**) ASK1, (**B**) c-Jun, and (**C**) ATF2 after treatment with Nano-PAC for 42 days.
Notes: Data are shown as mean±SD (n=6 rats/group). The bars with different letters (a–c) represent significant ($P<0.05$) difference as analyzed by the Duncan's multiple range test.
Abbreviations: Nano-PAC, PAC encapsulated in silica–chitosan nanoparticles; Con, control; DM, diabetes mellitus; Nano-PAC1, diabetes+4 mg/kg per day Nano-PAC; Nano-PAC2, diabetes+8 mg/kg per day Nano-PAC; Nano-PAC5, diabetes+20 mg/kg per day Nano-PAC; Met, diabetes+300 mg/kg per day metformin; Nano-con, diabetes+20 mg/kg per day silica–chitosan nanoparticles; PAC, petri dish-cultured *Antrodia cinnamomea*.

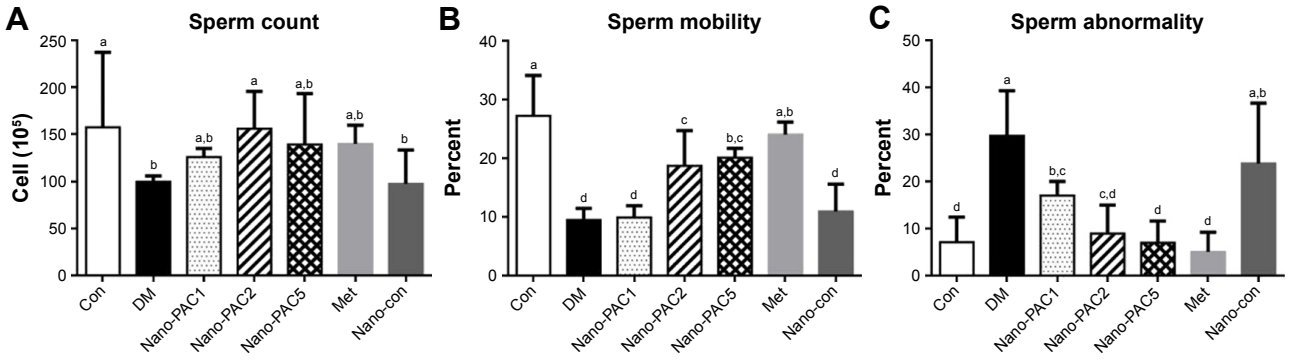

Figure 8 Sperm (**A**) count, (**B**) mobility, and (**C**) abnormality in STZ-induced diabetic rats fed different concentrations of Nano-PAC after 42 days.
Notes: Data are shown as mean±SD (n=6 rats/group). The bars with different letters (a–d) represent significant ($P<0.05$) difference as analyzed by the Duncan's multiple range test.
Abbreviations: STZ, streptozotocin; Nano-PAC, PAC encapsulated in silica–chitosan nanoparticles; Con, control; DM, diabetes mellitus; Nano-PAC1, diabetes+4 mg/kg per day Nano-PAC; Nano-PAC2, diabetes+8 mg/kg per day Nano-PAC; Nano-PAC5, diabetes+20 mg/kg per day Nano-PAC; Met, diabetes+300 mg/kg per day metformin; Nano-con, diabetes+20 mg/kg per day silica–chitosan nanoparticles; PAC, petri dish-cultured *Antrodia cinnamomea*.

was improved by treatment with Nano-PAC. Mitochondrion may be an important intracellular target for chemical-induced cell killing.[39] The Nano-PAC treatment successfully protects the sperm mitochondria.

Expression of testosterone, LH, and FSH in rat plasma

The effects of Nano-PAC treatment on STZ-induced diabetic rats were investigated. Figure 11 shows that the level

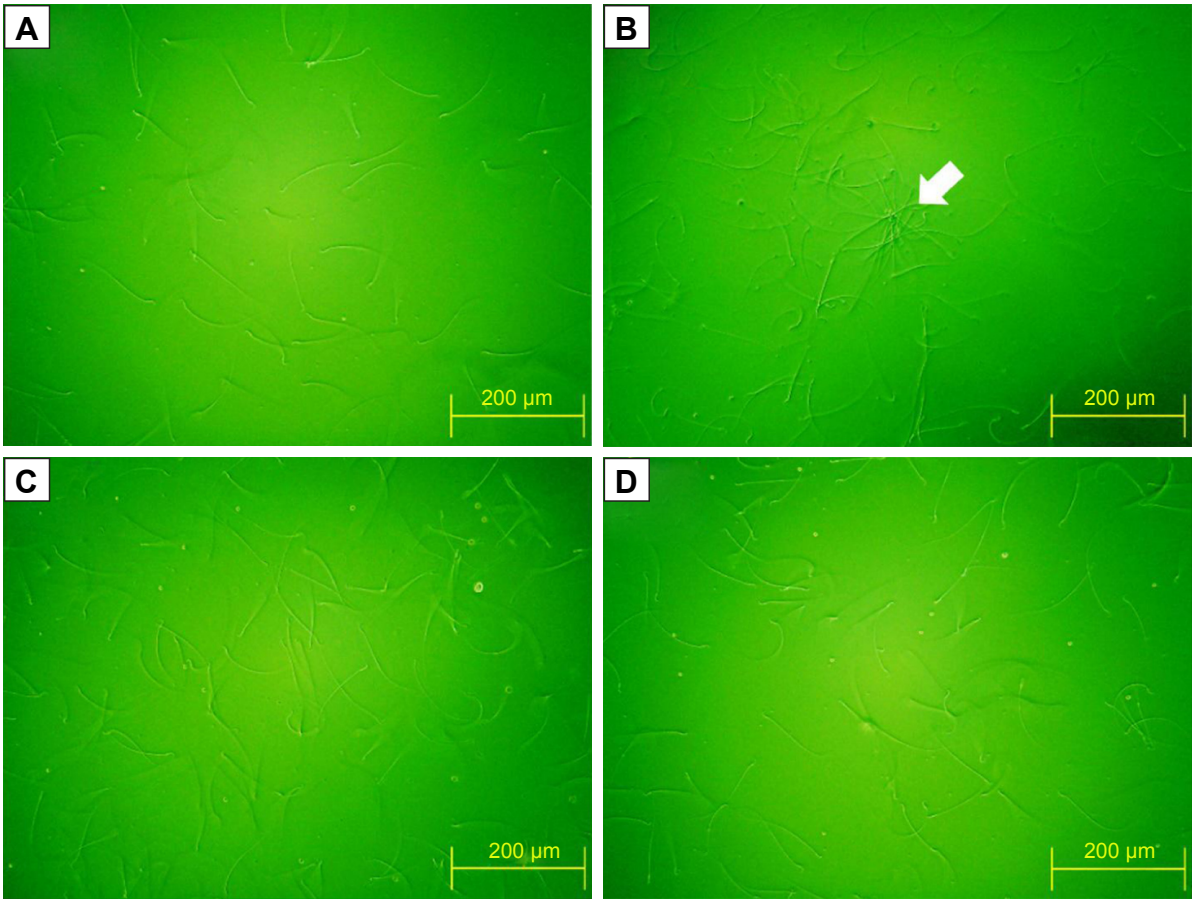

Figure 9 Sperm morphology of STZ-induced diabetic rats after 42 days fed Nano-PAC.
Notes: Light microscopy of sperm in each group (200×): (**A**) Con, (**B**) DM, (**C**) Nano-PAC5, and (**D**) Met. The white arrow represents abnormal sperm.
Abbreviations: STZ, streptozotocin; Nano-PAC, PAC encapsulated in silica–chitosan nanoparticles; Con, control; DM, diabetes mellitus; Nano-PAC5, diabetes+20 mg/kg per day Nano-PAC; Met, diabetes+300 mg/kg per day metformin; PAC, petri dish-cultured *Antrodia cinnamomea*.

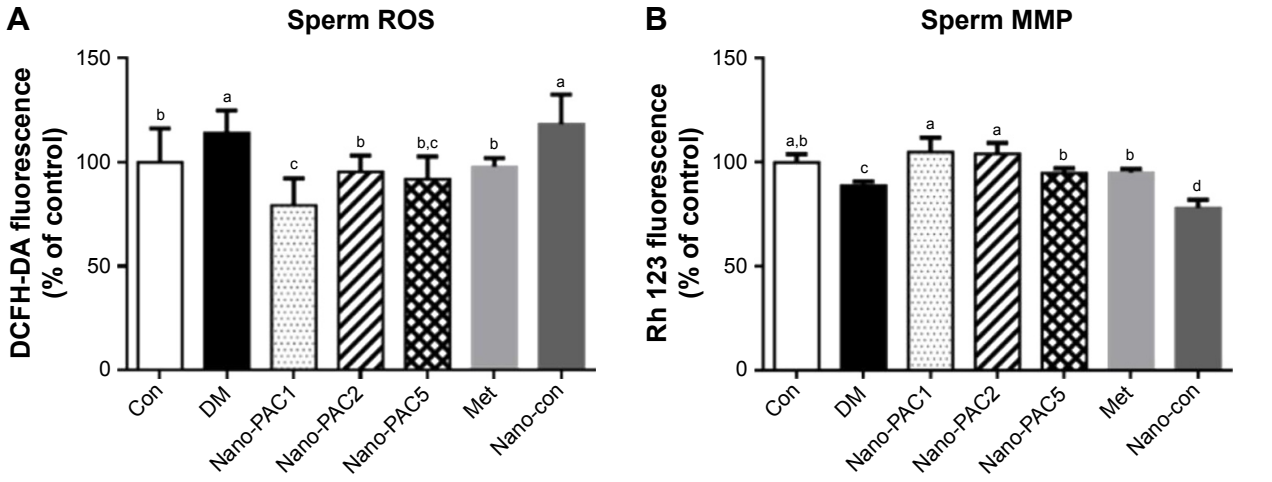

Figure 10 (**A**) ROS production and (**B**) the level of MMP of STZ-induced diabetes in sperm rats after fed Nano-PAC for 42 days.
Notes: Data are shown as mean±SD (n=6 rats/group). The bars with different letters (a–c) represent significant ($P<0.05$) difference as analyzed by the Duncan's multiple range test.
Abbreviations: MMP, mitochondrial membrane potential; STZ, streptozotocin; Nano-PAC, PAC encapsulated in silica–chitosan nanoparticles; Con, control; DM, diabetes mellitus; Nano-PAC1, diabetes+4 mg/kg per day Nano-PAC; Nano-PAC2, diabetes+8 mg/kg per day Nano-PAC; Nano-PAC5, diabetes+20 mg/kg per day Nano-PAC; Met, diabetes+300 mg/kg per day metformin; Nano-con, diabetes+20 mg/kg per day silica–chitosan nanoparticles; PAC, petri dish-cultured *Antrodia cinnamomea*; DCFH-DA, 2′,7′-dichlorofluorescein-diacetate; Rh 123, rhodamine 123; ROS, Reactive Oxygen Species.

of testosterone and LH when treated with Nano-PACs was significantly increased ($P<0.05$) compared with that in the diabetic (DM) group, whereas the FSH level significantly increased ($P<0.05$) when treated with Nano-PAC5 compared with that in the DM group.

In this study, testicular impairment in diabetic rats was indicated from declined circulating of testosterone, LH, and FSH expression. Diabetes has been reported to impair the circulating of LH and FSH levels, which severely affects androgen biosynthesis.[12,83] Hyperglycemia increases the resistance of the testis toward these hormones, leading to low testosterone levels.[84,85] Treatment of the diabetic rats with Nano-PACs has an ameliorated effect on the levels of testosterone, LH, and FSH.

NPs can improve the expression of FSH in testicular tissue than the control, but there is no significant difference. We hypothesize that Nano-PACs can protect the gonadotropic hormone such as FSH from the oxidative stress and can induce the expression of kisspeptin in the hypothalamic–pituitary–gonadal (HPG) axis. Kisspeptin is thought to exert its stimulatory effects on LH and FSH. The kisspeptin is released via the stimulation of GnRH from the hypothalamus.[86]

In addition, administration of Met (300 mg/kg) showed the amelioration effects as with Nano-PAC, especially Nano-PAC5 (20 mg/kg). At the end of the study, both of its treatments showed the improvements in STZ-induced diabetic rats, same as those in the Con group. In other hand,

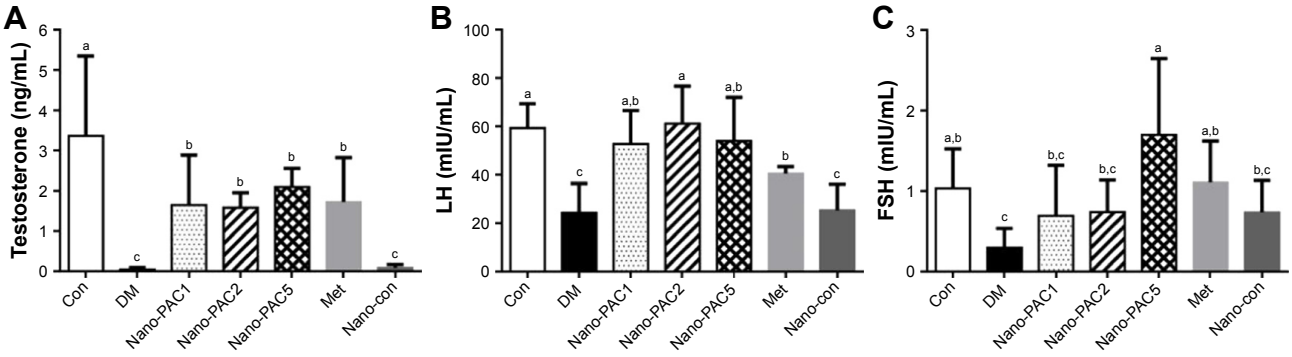

Figure 11 Expression of (**A**) testosterone, (**B**) LH, and (**C**) FSH in plasma of STZ-induced diabetic rats after treatment for 42 days.
Notes: Data are shown as mean±SD (n=6 rats/group). The bars with different letters (a–c) represent significant ($P<0.05$) difference as analyzed by the Duncan's multiple range test.
Abbreviations: LH, luteinizing hormone; FSH, follicle stimulating hormone; STZ, streptozotocin; Con, control; DM, diabetes mellitus; Nano-PAC1, diabetes+4 mg/kg per day Nano-PAC; Nano-PAC2, diabetes+8 mg/kg per day Nano-PAC; Nano-PAC5, diabetes+20 mg/kg per day Nano-PAC; Met, diabetes+300 mg/kg per day metformin; Nano-con, diabetes+20 mg/kg per day silica–chitosan nanoparticles; PAC, petri dish-cultured *Antrodia cinnamomea*.

administration with silica–chitosan NP (Nano-con) has not shown amelioration effects in diabetic rats. It is well known that triterpenoids from *A. cinnamomea* in Nano-PAC have high potent ameliorative properties in STZ-induced diabetic rats.

Conclusion

Our study successfully nanoencapsulated triterpenoids from *A. cinnamomea* with silica–chitosan to form NPs (Nano-PAC) with a small size and high EE. Oral administration of Nano-PAC shows beneficial effects in STZ-induced diabetic rats with ameliorated IR and oxidative stress. In addition to this, Nano-PAC regulated proinflammatory cytokines and testosterone, LH, and FSH as well as sperm and testis properties in diabetic rats as that in the Con group. Based on this result, Nano-PAC has potential to develop as an antidiabetic drug, targeted to regulate the male reproductive dysfunction with its high concentration.

Acknowledgment

This work was financially supported by the Center of Excellence for the Oceans, National Taiwan Ocean University from The Featured Areas Research Center Program within the framework of the Higher Education Sprout Project by the Ministry of Education (MOE) in Taiwan and MOST 106–2320-B-019–006.

Author contributions

Y-HH researched the articles and drafted the manuscript. AJ and DT participated in the manuscript design and coordination and drafted the manuscript. SS and Z-LK conceived the manuscript review, participated in its design and coordination, and drafted the manuscript. All authors contributed toward data analysis, drafting, and critically revising the paper; gave final approval of the version to be published; and agree to be accountable for all aspects of the work.

Disclosure

The authors report no conflicts of interest in this work.

References

1. Atta M, Almadaly E, El-Far A, et al. Thymoquinone Defeats Diabetes-Induced Testicular Damage in Rats Targeting Antioxidant, Inflammatory and Aromatase Expression. *Int J Mol Sci*. 2017;18(5):919.
2. Fatani AJ, Al-Rejaie SS, Abuohashish HM, Al-Assaf A, Parmar MY, Ahmed MM. Lutein Dietary Supplementation Attenuates Streptozotocin-induced testicular damage and oxidative stress in diabetic rats. *BMC Complement Altern Med*. 2015;15(1):204.
3. Asbun J, Villarreal FJ. The Pathogenesis of Myocardial Fibrosis in the Setting of Diabetic Cardiomyopathy. *J Am Coll Cardiol*. 2006;47(4):693–700.
4. Poitout V, Robertson RP. Minireview: Secondary β-Cell Failure in Type 2 Diabetes – A Convergence of Glucotoxicity and Lipotoxicity. *Endocrinology*. 2002;143(2):339–342.
5. Alsharari SD, Al-Rejaie SS, Abuohashish HM, Aleisa AM, Parmar MY, Ahmed MM. Ameliorative Potential of Morin in Streptozotocin-Induced Neuropathic Pain in Rats. *Tropical J of Pharmaceutical Res*. 2014;13(9):1429–1436.
6. Dogan Y, Akarsu S, Ustundag B, Yilmaz E, Gurgoze MK. Serum IL-1β, IL-2, and IL-6 in Insulin-dependent diabetic children. *Mediators Inflamm*. 2006;2006:1–6.
7. Abd El-Twab SM, Mohamed HM, Mahmoud AM. Taurine and pioglitazone attenuate diabetes-induced testicular damage by abrogation of oxidative stress and up-regulation of the pituitary–gonadal axis. *Can J Physiol Pharmacol*. 2016;94(6):651–661.
8. Aksu I, Baykara B, Kiray M, et al. Serum IGF-1 levels correlate negatively to liver damage in diabetic rats. *Biotech Histochem*. 2013;88(3–4):194–201.
9. Dandona P, Dhindsa S, Chandel A, Chaudhuri A. Hypogonadotropic Hypogonadism in Men with Type 2 Diabetes. *Postgrad Med*. 2009;121(3):45–51.
10. Guneli E, Tugyan K, Ozturk H, Gumustekin M, Cilaker S, Uysal N. Effect of Melatonin on Testicular Damage in Streptozotocin-Induced Diabetes Rats. *European Surgical Research*. 2008;40(4):354–360.
11. Agbaje IM, Rogers DA, Mcvicar CM, et al. Insulin dependant diabetes mellitus: implications for male reproductive function. *Hum Reprod*. 2007;22(7):1871–1877.
12. Ballester J, Muñoz MC, Domínguez J, Rigau T, Guinovart JJ, Rodríguez-Gil JE. Insulin-Dependent Diabetes Affects Testicular Function by FSH- and LH-Linked Mechanisms. *J Androl*. 2004;25(5):706–719.
13. Shrilatha B, Muralidhara. Early oxidative stress in testis and epididymal sperm in streptozotocin-induced diabetic mice: Its progression and genotoxic consequences. *Reprod Toxicol*. 2007;23(4):578–587.
14. Garber AJ, Abrahamson MJ, Barzilay JI, et al. Consensus Statement By The American Association Of Clinical Endocrinologists And American College Of Endocrinology On The Comprehensive Type 2 Diabetes Management Algorithm – *2017 Executive Summary*. *Endocr Pract*. 2017;23(2):207–238.
15. Thrasher J. Pharmacologic Management of Type 2 Diabetes Mellitus: Available Therapies. *Am J Cardiol*. 2017;120(1):S4–S16.
16. Wycherley TP, Noakes M, Clifton PM, Cleanthous X, Keogh JB, Brinkworth GD. A High-Protein Diet With Resistance Exercise Training Improves Weight Loss and Body Composition in Overweight and Obese Patients With Type 2 Diabetes. *Diabetes Care*. 2010;33(5):969–976.
17. Marín-Peñalver JJ, Martín-Timón I, Sevillano-Collantes C, Cañizo-Gómez Fjdel, Fjd C-G. Update on the treatment of type 2 diabetes mellitus. *World J Diabetes*. 2016;7(17):354–395.
18. Chaudhury A, Duvoor C, Reddy Dendi VS, et al. Clinical Review of Antidiabetic Drugs: Implications for Type 2 Diabetes Mellitus Management. *Front Endocrinol*. 2017;8(Suppl 1).
19. Chang TT, Chou WN. *Antrodia cinnamomea* sp. nov. on *Cinnamomum kanehirai* in Taiwan. *Mycol Res*. 1995;99(6):756–758.
20. Geethangili M, Tzeng Y-M. Review of Pharmacological Effects of *Antrodia camphorata* and Its Bioactive Compounds. *Evidence-Based Complementary and Alternative Medicine*. 2011;2011(6):1–17.
21. Huang T-H, Chiu Y-H, Chan Y-L, et al. *Antrodia cinnamomea* alleviates cisplatin-induced hepatotoxicity and enhances chemo-sensitivity of line-1 lung carcinoma xenografted in BALB/cByJ mice. *Oncotarget*. 2015;6(28):25741–25754.
22. Chang C-J, Lu C-C, Lin C-S, et al. *Antrodia cinnamomea* reduces obesity and modulates the gut microbiota in high-fat diet-fed mice. *Int J Obes*. 2018;42(2):231–243.
23. Huang T-T, Wu S-P, Chong K-Y, et al. The medicinal fungus *Antrodia cinnamomea* suppresses inflammation by inhibiting the NLRP3 inflammasome. *J Ethnopharmacol*. 2014;155(1):154–164.
24. Lin C-H, Kuo Y-H, Shih C-C. Eburicoic Acid, a Triterpenoid Compound from *Antrodia camphorata*, Displays Antidiabetic and Antihyperlipidemic Effects in Palmitate-Treated C2C12 Myotubes and in High-Fat Diet-Fed Mice. *Int J Mol Sci*. 2017;18(11):2314.

25. Valdés K, Morales J, Rodríguez L, Günther G. Potential use of nanocarriers with pentacyclic triterpenes in cancer treatments. *Nanomedicine*. 2016;11(23):3139–3156.
26. Jeong DW, Kim YH, Kim HH, et al. Dose-linear pharmacokinetics of oleanolic acid after intravenous and oral administration in rats. *Biopharm Drug Dispos*. 2007;28(2):51–57.
27. Yin M-C, Lin M-C, Mong M-C, Lin C-Y. Bioavailability, Distribution, and Antioxidative Effects of Selected Triterpenes in Mice. *J Agric Food Chem*. 2012;60(31):7697–7701.
28. Jin H, Pi J, Yang F, et al. Folate-Chitosan Nanoparticles Loaded with Ursolic Acid Confer Anti-Breast Cancer Activities in vitro and in vivo. *Sci Rep*. 2016;6(1).
29. Wilczewska AZ, Niemirowicz K, Markiewicz KH, Car H. Nanoparticles as drug delivery systems. *Pharmacological Reports*. 2012;64(5):1020–1037.
30. Suri S, Fenniri H, Singh B. Nanotechnology-based drug delivery systems. *J Occup Med Toxicol*. 2007;2(1):16.
31. Kong Z-L, Chang J-S, Chang KLB. Antiproliferative effect of *Antrodia camphorata* polysaccharides encapsulated in chitosan–silica nanoparticles strongly depends on the metabolic activity type of the cell line. *Journal of Nanoparticle Research*. 1945;2013(15(9).
32. Zhang Z, Feng S-S. The drug encapsulation efficiency, in vitro drug release, cellular uptake and cytotoxicity of paclitaxel-loaded poly(lactide)–tocopheryl polyethylene glycol succinate nanoparticles. *Biomaterials*. 2006;27(21):4025–4033.
33. Maiti S, Jana S, Laha B. Cationic polyelectrolyte–biopolymer complex hydrogel particles for drug delivery. In. *Design and Development of New Nanocarriers*; 2018:223–256.
34. van de Loosdrecht AA, Beelen RHJ, Ossenkoppele GJ, Broekhoven MG, Langenhuijsen MMAC. A tetrazolium-based colorimetric MTT assay to quantitate human monocyte mediated cytotoxicity against leukemic cells from cell lines and patients with acute myeloid leukemia. *J Immunol Methods*. 1994;174(1–2):311–320.
35. Sim Choi H, Woo Kim J, Cha Young-nam, Kim C, Choi HS, Kim JW, Cha YN. A Quantitative Nitroblue Tetrazolium Assay for Determining Intracellular Superoxide Anion Production in Phagocytic Cells. *Journal Immunoassay and Immunochemistry*. 2006;27(1):31–44.
36. Abdelali Alà, Al-Bader M, Kilarkaje N. Effects of Trans-Resveratrol on hyperglycemia-induced abnormal spermatogenesis, DNA damage and alterations in poly (ADP-ribose) polymerase signaling in rat testis. *Toxicol Appl Pharmacol*. 2016;311:61–73.
37. Collodel G, Federico MG, Geminiani M, et al. Effect of trans-resveratrol on induced oxidative stress in human sperm and in rat germinal cells. *Reprod Toxicol*. 2011;31(2):239–246.
38. Abbasihormozi S, Shahverdi A, Kouhkan A, Cheraghi J, Akhlaghi AA, Kheimeh A. Relationship of leptin administration with production of reactive oxygen species, sperm DNA fragmentation, sperm parameters and hormone profile in the adult rat. *Arch Gynecol Obstet*. 2013;287(6):1241–1249.
39. Palmeira CM, Moreno AJM, Madeira VMC, Wallace KB. Continuous monitoring of mitochondrial membrane potential in hepatocyte cell suspensions. *J Pharmacol Toxicol Methods*. 1996;35(1):35–43.
40. Hu J-F, Li S-F, Raghavan Nair G, Wu W-T. Predicting chitosan particle size produced by electrohydrodynamic atomization. *Chem Eng Sci*. 2012;82:159–165.
41. Atalay S, Barisik M, Beskok A, Qian S. Surface Charge of a Nanoparticle Interacting with a Flat Substrate. *J Phys Chem C*. 2014;118(20):10927–10935.
42. Chithrani BD, Ghazani AA, Chan WCW. Determining the Size and Shape Dependence of Gold Nanoparticle Uptake into Mammalian Cells. *Nano Lett*. 2006;6(4):662–668.
43. Xie X, Liao J, Shao X, Li Q, Lin Y. The Effect of shape on Cellular Uptake of Gold Nanoparticles in the forms of Stars, Rods, and Triangles. *Sci Rep*. 2017;7(1).
44. Bharathiraja S, Manivasagan P, Quang Bui N, et al. Cytotoxic Induction and Photoacoustic Imaging of Breast Cancer Cells Using Astaxanthin-Reduced Gold Nanoparticles. *Nanomaterials*. 2016;6(4):78.
45. Salatin S, Yari Khosroushahi A. Overviews on the cellular uptake mechanism of polysaccharide colloidal nanoparticles. *J Cell Mol Med*. 2017;21(9):1668–1686.
46. Dong Y, Feng S-S. Methoxy poly(ethylene glycol)-poly(lactide) (MPEG-PLA) nanoparticles for controlled delivery of anticancer drugs. *Biomaterials*. 2004;25(14):2843–2849.
47. Kuhn DA, Vanhecke D, Michen B, et al. Different endocytotic uptake mechanisms for nanoparticles in epithelial cells and macrophages. *Beilstein J Nanotechnol*. 2014;5:1625–1636.
48. Atalay S, Ma Y, Qian S. Analytical model for charge properties of silica particles. *J Colloid Interface Sci*. 2014;425:128–130.
49. Wang H, Agarwal P, Zhao S, Yu J, Lu X, He X. A biomimetic hybrid nanoplatform for encapsulation and precisely controlled delivery of theranostic agents. *Nat Commun*. 2015;6(1).
50. Zhao J, Lu H, Wong S, Lu M, Xiao P, Stenzel MH. Influence of nanoparticle shapes on cellular uptake of paclitaxel loaded nanoparticles in 2D and 3D cancer models. *Polym Chem*. 2017;8(21):3317–3326.
51. Champion JA, Katare YK, Mitragotri S. Particle shape: A new design parameter for micro- and nanoscale drug delivery carriers. *Journal of Controlled Release*. 2007;121(1–2):3–9.
52. Simone EA, Dziubla TD, Muzykantov VR. Polymeric carriers: role of geometry in drug delivery. *Expert Opin Drug Deliv*. 2008;5(12):1283–1300.
53. Shimoni O, Yan Y, Wang Y, Caruso F. Shape-Dependent Cellular Processing of Polyelectrolyte Capsules. *ACS Nano*. 2013;7(1):522–530.
54. Mittal M, Siddiqui MR, Tran K, Reddy SP, Malik AB. Reactive Oxygen Species in Inflammation and Tissue Injury. *Antioxid Redox Signal*. 2014;20(7):1126–1167.
55. Sharma JN, Al-Omran A, Parvathy SS. Role of nitric oxide in inflammatory diseases. *Inflammopharmacology*. 2007;15(6):252–259.
56. Chang KJ, Kwon W. Immunohistochemical localization of insulin in pancreatic β-Cells of taurine-supplemented or taurine-depleted diabetic rats. *Adv Exp Med Biol*. 2002;4:579–587.
57. Pandya KG, Patel MR, Lau-Cam CA. Comparative study of the binding characteristics to and inhibitory potencies towards PARP and in vivo antidiabetogenic potencies of taurine, 3-aminobenzamide and nicotinamide. *J Biomed Sci*. 2010;17(Suppl 1):S16.
58. Kuo Y-H, Lin C-H, Shih C-C, Yang C-S. Antcin K, a Triterpenoid Compound from *Antrodia camphorata*, Displays Antidiabetic and Antihyperlipidemic Effects via Glucose Transporter 4 and AMP-Activated Protein Kinase Phosphorylation in Muscles. *Evid Based Complementary and Alternat Medicine*. 2016;2016(1):1–16.
59. Kuo Y-H, Lin C-H, Shih C-C. Antidiabetic and Antihyperlipidemic Properties of a Triterpenoid Compound, Dehydroeburicoic Acid, from *Antrodia camphorata* in Vitro and in Streptozotocin-Induced Mice. *J Agric Food Chem*. 2015;63(46):10140–10151.
60. Qu HQ, Li Q, Rentfro AR, Fisher-Hoch SP, Mccormick JB. The definition of insulin resistance using HOMA-IR for Americans of Mexican descent using Machine Learning. *PLoS One*. 2011;6(6):e21041.
61. Gayoso-Diz P, Otero-González A, Rodriguez-Alvarez MX, et al. Insulin resistance (HOMA-IR) cut-off values and the metabolic syndrome in a general adult population: effect of gender and age: EPIRCE cross-sectional study. *BMC Endocr Disord*. 2013;13(1).
62. Kim J-A, Montagnani M, Koh KK, Quon MJ. Reciprocal Relationships Between Insulin Resistance and Endothelial Dysfunction: Molecular and Pathophysiological Mechanisms. *Circulation*. 2006;113(15):1888–1904.
63. Geloneze B, Repetto EM, Geloneze SR, Tambascia MA, Ermetice MN. The threshold value for insulin resistance (HOMA-IR) in an admixtured population. *Diabetes Res Clin Pract*. 2006;72(2):219–220.
64. Yashpal S, Mk G, Nikhil T, Kumar MR. A Study of Insulin Resistance by HOMA-IR and its Cut-off Value to Identify Metabolic Syndrome in Urban Indian Adolescents. *J Clin Res Pediatr Endocrinol*. 2013;5(4):245–251.
65. Soudamani S, Yuvaraj S, Malini T, Balasubramanian K. Experimental diabetes has adverse effects on the differentiation of ventral prostate during sexual maturation of rats. *Anat Rec A Discov Mol Cell Evol Biol*. 2005;287A(2):1281–1289.

66. O'Donnell L, Mclachlan RI, Wreford NG, Robertson DM. Testosterone promotes the conversion of round spermatids between stages VII and VIII of the rat spermatogenic cycle. *Endocrinology*. 1994; 135(6):2608–2614.
67. Bjørndal B, Burri L, Staalesen V, Skorve J, Berge RK. Different Adipose Depots: Their Role in the Development of Metabolic Syndrome and Mitochondrial Response to Hypolipidemic Agents. *J Obes*. 2011; 2011(1):1–15.
68. Orman D, Vardi N, Ates B, Taslidere E, Elbe H. Aminoguanidine mitigates apoptosis, testicular seminiferous tubules damage, and oxidative stress in streptozotocin-induced diabetic rats. *Tissue Cell*. 2015;47(3): 284–290.
69. Sisman AR, Kiray M, Camsari UM, et al. Potential Novel Biomarkers for Diabetic Testicular Damage in Streptozotocin-Induced Diabetic Rats: Nerve Growth Factor Beta and Vascular Endothelial Growth Factor. *Dis Markers*. 2014;2014(4):1–7.
70. Cui X-P, Li B-Y Gh-Q, Wei N, W-L W, Lu M. Effects of grape seed proanthocyanidin extracts on peripheral nerves in streptozocin-induced diabetic rats. *J Nutr Sci Vitaminol*. 2008;54(4):321–328.
71. Faid I, Al-Hussaini H, Kilarkaje N. Resveratrol alleviates diabetes-induced testicular dysfunction by inhibiting oxidative stress and c-Jun N-terminal kinase signaling in rats. *Toxicol Appl Pharmacol*. 2015; 289(3):482–494.
72. Kushwaha S, Jena GB. Telmisartan ameliorates germ cell toxicity in the STZ-induced diabetic rat: Studies on possible molecular mechanisms. *Mutat Res/Genet Toxicol Environ Mutagen*. 2013;755(1):11–23.
73. Fachinan R, Yessoufou A, Nekoua MP, Moutairou K. Effectiveness of Antihyperglycemic Effect of *Momordica charantia*: Implication of T-Cell Cytokines. *Evid Based Complement Alternat Med*. 2017;2017(12):1–8.
74. Brownlee M. The Pathobiology of Diabetic Complications: A Unifying Mechanism. *Diabetes*. 2005;54(6):1615–1625.
75. Navarro-Gonzalez JF, Mora-Fernandez C. The Role of Inflammatory Cytokines in Diabetic Nephropathy. *J Am Soc Nephrol*. 2008;19(3):433–442.
76. Haim Y, Blüher M, Konrad D, et al. ASK1 (MAP3K5) is transcriptionally upregulated by E2F1 in adipose tissue in obesity, molecularly defining a human dys-metabolic obese phenotype. *Mol Metab*. 2017; 6(7):725–736.
77. Miyata Y, Fukuhara A, Otsuki M, Shimomura I. Expression of Activating Transcription Factor 2 in Inflammatory Macrophages in Obese Adipose Tissue. *Obesity*. 2012;112.
78. Bhoumik A, Lopez-Bergami P, Ronai Z. ATF2 on the double – activating transcription factor and DNA damage response protein. *Pigment Cell Res*. 2007;20(6):498–506.
79. Solinas G, Becattini B. JNK at the crossroad of obesity, insulin resistance, and cell stress response. *Mol Metab*. 2017;6(2):174–184.
80. Kilarkaje N, Al-Hussaini H, Al-Bader MM. Diabetes-induced DNA damage and apoptosis are associated with poly (ADP ribose) polymerase 1 inhibition in the rat testis. *Eur J Pharmacol*. 2014;737:29–40.
81. Song T-Y, Yen G-C. Antioxidant Properties of *Antrodia camphorata* in Submerged Culture. *J Agric Food Chem*. 2002;50(11):3322–3327.
82. Wang J-J, Wu C-C, Lee C-L, Hsieh S-L, Chen J-B, Lee C-I. Antimelanogenic, Antioxidant and Antiproliferative Effects of Antrodia camphorata Fruiting Bodies on B16-F0 Melanoma Cells. *PLoS One*. 2017; 12(1):e0170924.
83. Schoeller EL, Schon S, Moley KH. The effects of type 1 diabetes on the hypothalamic, pituitary and testes axis. *Cell Tissue Res*. 2012;349(3): 839–847.
84. Khaki A, Fathiazad F, Nouri M, et al. Beneficial effects of quercetin on sperm parameters in streptozotocin-induced diabetic male rats. *Phytotherapy Research*. 2010;24(9):1285–1291.
85. Navarro-Casado L, Juncos-Tobarra MA, Chafer-Rudilla M, de Onzono LI, Blazquez-Cabrera JA, Miralles-Garcia JM. Effect of Experimental Diabetes and STZ on Male Fertility Capacity. Study in Rats. *J Androl*. 2010;31(6):584–592.
86. Abbara A, Ratnasabapathy R, Jayasena CN, Dhillo WS. The effects of kisspeptin on gonadotropin release in non-human mammals. In: *Kisspeptin Signaling in Reproductive Biology*; 2013(784):63–87.